

No. 65 - 003

Stability of a Shear Flow in an
Unstable Layer

Thomas J. Eisler

Department of Space Science and Applied Physics
The Catholic University of America
Washington, D. C.

January, 1965

Abstract

21355

The stability with respect to small perturbations of a piecewise linear velocity profile of the half-jet (or shear layer) type in a layer with an unstable entropy gradient has been studied. The maximum instabilities are found to be either in the plane of the velocity profile or perpendicular to it depending on a critical Richardson number which is quite insensitive to the depth of the layer.

Arthur

Stability of a Shear Flow in an

Unstable Layer

Thomas J. Eisler

The Catholic University of America

Washington, D. C.

I. INTRODUCTION

Previous studies of the stability of a shear flow in a thermally unstable atmosphere have been restricted to velocity profiles with constant shear.¹⁻³ This combination of unstable stratification with a stable velocity profile has been used as a model for the atmosphere, and in particular, has been used to explain frequently observed cloud formations in unstable layers which take the form of long rolls with their axes parallel to the wind direction¹. In such a model these are the only motions which are not affected by the inhibiting effect of the shear. One of the difficulties of such a model is that it does not establish the width of the rolls since the maximum instability occurs for infinite wave number. Moreover, it has been observed that a vertical variation of shear in the unstable layer seems to be characteristic of these formations⁴, and it seems clear that, at least for ^asufficiently small (negative) Richardson number, the instabilities of such a velocity profile should dominate.

In general, when both types of instability are present, one might expect the maximum instability to represent an interaction between them (especially in view of the inequality (3.1) derived in section 3) occurring for a finite wave number which would establish the scale of the motion. To include the effect of a variable shear, a piecewise linear profile has been used in a layer with a negative entropy gradient. The results for this simple model are negative, i.e., instabilities are either of the

shear type or the convective type depending on a critical Richardson number but no interaction is found. This does not, of course, exclude the possibility of such an interaction for a more realistic model.

2. THE PERTURBATION EQUATIONS

The fundamental equations to be used are the momentum and continuity equations, the conservation of entropy, and the perfect gas law:

$$\frac{D \vec{v}_*}{D t_*} + \frac{1}{\rho_*} \text{grad } p_* + \vec{g} = 0$$

$$\frac{D \rho_*}{D t_*} + \rho_* \text{div } \vec{v}_* = 0$$

$$\frac{D S_*}{D t_*} = 0$$

$$p_* = (\text{constant}) e^{\frac{S_* / c_v}{\rho_*} \gamma}$$

Asterisks are used to denote dimensional quantities. The gravitational constant is g and \vec{g} is $(0,0,g)$. The quantities V_* , ρ_* , p_* , and S_* are the velocity, density, pressure, and entropy, and γ is the ratio of specific heats, C_p/C_v . These equations are linearized about a mean velocity $(U(z), 0, 0)$, and a mean density, pressure, and entropy $\bar{\rho}_*(z)$, $\bar{p}_*(z)$ and $\bar{S}_*(z)$ by the equations

$$\vec{V}_* = (u_* + u'_*, v'_*, w'_*)$$

$$\rho_* = \bar{\rho}_* + \rho'_*$$

$$p_* = \bar{p}_* + p'_*$$

$$s_* = \bar{s}_* + s'_*$$

where the primed quantities are assumed small. If we assume that the primed quantities have the form

$$g' = g(z) e^{i(\alpha_* x + \beta_* y - \alpha_* c_* t_*)}$$

and if we further neglect acoustic waves by setting the velocity of sound,

$\sqrt{\gamma p_*/\rho_*}$, equal to infinity and solve the linearized equations for W we obtain the equation

$$W_*'' + \frac{\rho'_*}{\rho_*} W_*' + W_* \left\{ -\frac{\rho'_*}{\rho_*} \frac{u'_*}{u_* - c_*} - \frac{u_*''}{u_* - c_*} - k_*^2 \left(1 - \frac{g(s'_*/c_p)}{\alpha_*^2 (u_* - c_*)^2} \right) \right\} = 0 \quad (2.1)$$

where k_* is the total wave number

$$k_*^2 = \alpha_*^2 + \beta_*^2$$

Here, primes denote derivatives with respect to z .

We next make the Boussinesq approximation of neglecting the variation of density, except where it is multiplied by the gravitational constant g . The resulting equation can be put into dimensionless form by introducing reference quantities V, ρ_0 for the

velocity and density and by assuming that the velocity field is characterized by a length l and that the stratification is characterized by a length d . We obtain

$$W'' - \left\{ K^2 + \frac{U''}{U-C} - \frac{K^2}{\alpha^2} \frac{J}{(U-C)^2} \right\} W = 0 \quad (2.2)$$

where the asterisks are dropped to denote dimensionless quantities. J is the local Richardson number given by

$$J = \frac{g l^2}{v^2 d} \frac{S'}{c_p}$$

3. A BOUND ON THE AMPLIFICATION OF THE PERTURBATIONS

A method of Howard⁵ can be used to obtain a bound on the complex wave velocity, c_* , of three dimensional amplified perturbations. Acoustic waves are neglected but the Boussinesq approximation is not needed. Equation (2.1) can be written

$$\left[\rho_* (U_* - c_*) F' \right]' + \rho_* \left[\frac{K_*^2}{\alpha_*^2} g \frac{S'_*}{c_p} - K_*^2 (U_* - c_*)^2 \right] F = 0$$

where

$$F = \frac{W_*}{U_* - c_*}$$

If we multiply by the complex conjugate of F , integrate over (z_1, z_2) (where z_1 and z_2 may become infinite), and impose $F = 0$ at z_1 and z_2 , we obtain

$$\int dz \rho_* (U_* - c_*)^2 Q - \int dz g \frac{S'_*}{c_p} |F|^2 \rho_* = 0$$

where

$$Q = \rho_* \left\{ |F'|^2 + K_*^2 |F|^2 \right\}$$

If this equation is separated into real and imaginary parts, from the imaginary part we have, assuming $c_i > 0$,

$$\int dz U_* Q = c_{n*} \int dz Q$$

The real part can now be written

$$\int dz U_*^2 Q = (c_{n*}^2 + c_{i*}^2) \int dz Q + \int dz \frac{k_*^2}{\alpha_*^2} \frac{s_*'}{c_p} g \rho_* |F|^2$$

If $a \leq U_*(z) \leq b$ then

$$0 \geq \int dz (U_* - a)(U_* - b) Q =$$

$$\left\{ \left(c_{n*} - \frac{a+b}{2} \right)^2 + c_{i*}^2 - \left(\frac{a-b}{2} \right)^2 \right\} \int dz Q + \int dz \frac{k_*^2}{\alpha_*^2} \frac{s_*'}{c_p} g \rho_* |F|^2$$

and

$$\left(c_{n*} - \frac{a+b}{2} \right)^2 + c_{i*}^2 \leq \left(\frac{a-b}{2} \right)^2 - \frac{\int dz \frac{s_*'}{c_p} \frac{k_*^2}{\alpha_*^2} g \rho_* |F|^2}{\int dz \rho_* \{ |F'|^2 + k_*^2 |F|^2 \}}$$

We assume that the entropy gradient is negative. Let $(-g \frac{s_*'}{c_p})_{\max}$ be the maximum of $-g \frac{s_*'}{c_p}$ in (z_1, z_2) . Then

$$\begin{aligned} \left(c_{n*} - \frac{a+b}{2} \right)^2 + c_{i*}^2 &\leq \left(\frac{a-b}{2} \right)^2 - \frac{\left(g \frac{s_*'}{c_p} \right)_{\max} \frac{k_*^2}{\alpha_*^2}}{k_*^2 + \frac{\int dz \rho_* |F'|^2}{\int dz \rho_* |F|^2}} \\ &\leq \left(\frac{a-b}{2} \right)^2 - \frac{1}{\alpha_*^2} \left(g \frac{s_*'}{c_p} \right)_{\max} \end{aligned}$$

Thus, c_* is restricted to a semicircle in the complex c_* - plane whose center is the midpoint of the range of U_* . If we assume (without loss of generality) that

$-U_{0*} \leq U_*(z) \leq U_{0*}$, then in dimensionless form this becomes

$$|\alpha c|^2 \leq \alpha^2 U_0^2 - J_{max} \quad (3.1)$$

The first term on the right hand side of (3.1) is the maximum amplification for a shear flow alone while the second term is the maximum amplification for an unstable layer. Thus, the inequality suggests the possibility of an amplification for the combined effect of the two types of instability which is greater than that due to either cause by itself.

4. THE EIGENVALUE EQUATION

We assume a dimensionless velocity profile:

$$U = z \quad |z| \leq 1$$

$$U = \pm 1 \quad |z| \geq 1$$

and an unstable layer $|z| < L$:

$$J < 0 \quad |z| < L$$

$$J = 0 \quad |z| > L$$

where $L = d/\rho \geq 1$ (Figure 1)

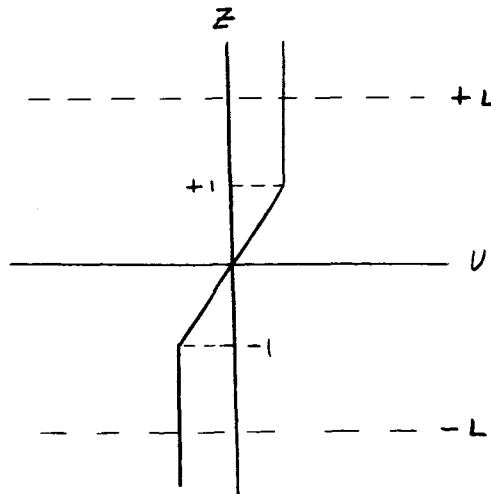


Figure 1

Solutions of Eq. (2.2) are easily obtained as exponentials for $|z| > 1$.

Let the solutions of Eq. (2.2) be W_1 and W_2 for $|z| < 1$. Then W_1 and W_2 have the form

$$\sqrt{i(z-c)} Z_n(i(z-c))$$

where Z_n is a Bessel function of order n . The index n is given by $n^2 = \frac{1}{4} - \frac{J}{\cos^2 \theta}$ where θ is the angle which the wave number of the perturbation, k , makes with the x -axis (thus, $\alpha = k \cos \theta$).

Imposing the continuity of W and W' at $\pm L$ and at ± 1 the continuity of W and the jump conditions

$$\left[\frac{dW}{dz} \right]_{z=1} = \frac{W(1)}{1-c}$$

$$\left[\frac{dW}{dz} \right]_{z=-1} = \frac{W(-1)}{1+c}$$

where the square brackets denote the jump in crossing the interface in the positive sense, we obtain the eigenvalue equation for c :

$$\begin{aligned} & \frac{(iS_+) W_1'(iS_+) - W_1(iS_+) \left\{ 1 - \sqrt{S_+^2 + n^2 - \frac{1}{4}} \right\} \frac{K + K_+ \tanh K_+ (L-1)}{K_+ + K \tanh K_+ (L-1)}}{(iS_+) W_2'(iS_+) - W_2(iS_+) \left\{ 1 - \sqrt{S_+^2 + n^2 - \frac{1}{4}} \right\} \frac{K + K_+ \tanh K_+ (L-1)}{K_+ + K \tanh K_+ (L-1)}} \\ &= \frac{(iS_-) W_1'(iS_-) - W_1(iS_-) \left\{ 1 + \sqrt{S_-^2 + n^2 - \frac{1}{4}} \right\} \frac{K + K_- \tanh K_- (L-1)}{K_- + K \tanh K_- (L-1)}}{(iS_-) W_2'(iS_-) - W_2(iS_-) \left\{ 1 + \sqrt{S_-^2 + n^2 - \frac{1}{4}} \right\} \frac{K + K_- \tanh K_- (L-1)}{K_- + K \tanh K_- (L-1)}} \end{aligned}$$

Here the primes denote derivatives of W_1 and W_2 with respect to their arguments (not with respect to z) and

$$S_+ = K (1 - c)$$

$$S_- = -K (1 + c)$$

$$K_+ = \frac{K}{S_+} \sqrt{S_+^2 + \eta^2 - \frac{1}{4}}$$

$$K_- = \frac{K}{S_-} \sqrt{S_-^2 + \eta^2 - \frac{1}{4}}$$

The branch cuts of the square root functions are defined so that they have a positive real part.

5. THE CASE $L = 1$

Equation (4.1) is considerably simplified if we set $L = 1$:

$$\frac{(iS_+) W_1'(iS_+) + (S_+ - 1) W_1(iS_+)}{(iS_+) W_2'(iS_+) + (S_+ - 1) W_2(iS_+)} = \frac{(iS_-) W_1'(iS_-) - (S_- + 1) W_1(iS_-)}{(iS_-) W_2'(iS_-) - (S_- + 1) W_2(iS_-)} \quad (5.1)$$

It can, therefore, be studied in greater detail and the results seem to be qualitatively the same as for the case $L > 1$.

(a) Expansion in Powers of the Wave Number

Assuming that the total wave number, k , is small, and that S_+ and S_- are of the order of magnitude of k , we may expand W_1 and W_2 in Eq. (5.1) in power series. The first approximation gives

$$\left(\frac{S_+}{S_-} \right)^{2n} = 1 = e^{2\pi i l} \quad (l = \text{integer})$$

The assumption $c_i > 0$ implies that

$$-\pi < \arg \frac{S_+}{S_-} < \pi$$

and, therefore, that

$$-n < l < n$$

To the second order we obtain

$$C = i \cot \frac{l\pi}{2n} \left\{ 1 - \frac{2}{n^2 - 1/4} \frac{K}{1 - \cos \pi l/n} + O(K^2) \right\} \quad 0 < l < n$$

where a further restriction on l is made to avoid violating our assumptions $c_i > 0$ and S_+, S_- of order k .

Another solution can be found by assuming that kc is of the order of magnitude of \sqrt{k} . We find

$$C = i \left\{ \sqrt{\frac{n^2 - 1/4}{K}} - \frac{1}{3} \frac{n^2 - 7/4}{\sqrt{n^2 - 1/4}} \sqrt{K} + O(K^{3/2}) \right\}$$

Thus, we have found $[n] + 1$ amplified modes, where $[n]$ is the greatest integer in n . This is not necessarily the total number of such modes. In fig. 2, for example, it is seen that for $n = 0.9$ there are two modes, one of which exists only for $k \geq 0.53$. When n is half of an odd integer, however, it can be shown that $[n] + 1$ is the total number of amplified modes (see part (c)).

Figure 2

$$n = 0.9 \quad L = 1$$

(b) Expansions for Large Values of the Wave Number

If we assume that both S_+ and S_- are of the order of magnitude of k as $k \rightarrow \infty$ and use the asymptotic expansions for W_1 and W_2 in Eq. (5.1), we are led to an impossibility. Thus, it is clear that $c \rightarrow \pm 1$ as $k \rightarrow \infty$. This is not surprising since to very small wavelengths the configuration should look roughly like a pair of flow regimes each consisting of two linear profiles extending to infinity.

Using $H_n^{(1)}$ and $H_n^{(2)}$ as the solutions of Bessel's equation and the asymptotic expansions for $W_1(i S_-)$, $W_2(i S_-)$ as $c \rightarrow 1$ and the asymptotic expansions for $W_1(i S_+)$, $W_2(i S_+)$ as $c \rightarrow -1$, in the limit of infinite k we obtain the pair of equations

$$i S_+ H_n^{(2)'}(i S_+) + (S_+ - \frac{1}{2}) H_n^{(2)}(i S_+) = 0$$

$$i S_- H_n^{(1)'}(i S_-) - (S_- + \frac{1}{2}) H_n^{(1)}(i S_-) = 0$$

Thus, for infinite k we obtain two completely decoupled waves.

These equations are easily solved for half integer values of n for then they become polynomials of order $\frac{2n+1}{2}$. For example, for $n = 3/2$ we obtain four solutions

$$c = \pm \left\{ 1 - \frac{3/4 \pm i \sqrt{7}/4}{k} \right\}$$

$$\alpha c_i = \pm 0.468 \sqrt{J}$$

and for $n = 5/2$ we obtain six solutions

$$c = \pm \left\{ 1 - \frac{3/2}{k} \right\} \quad \alpha c_i = 0$$

$$c = \pm \left\{ 1 - \frac{1 \pm i \sqrt{2}}{k} \right\} \quad \alpha c_i = \pm 0.585 \sqrt{J}$$

As we shall see in the next section, one of the peculiarities of these solutions is that the amplification factor $\propto c_1$ is essentially constant over the entire range where $c_r \neq 0$

(c) Solutions for Half Integer Values of n

When n is half of an odd integer the Bessel functions can be written in terms of elementary functions and Eq. (5.1) can be written in terms of $S_+ S_- = -k^2(1 - c^2)$ and $S_+ - S_- = 2k$; in fact, it is a polynomial of order $\frac{2n+1}{2}$ in $S_+ S_-$. For example, for $n = 3/2$ we have

$$(S_+ S_-)^2 + S_+ S_- \left\{ 3K - \frac{1}{4} + \frac{1}{4} e^{-4K} \right\} + 4K^2 - 3K + 1 - e^{-4K} (K+1) = 0$$

and for $n = 5/2$ we have

$$(S_+ S_-)^3 + (S_+ S_-)^2 \left\{ 7K - \frac{1}{4} + \frac{1}{4} e^{-4K} \right\} + (S_+ S_-) \left\{ 24K^2 - 15K + \frac{9}{2} - e^{-4K} \left(3K + \frac{9}{2} \right) \right\} + 36K^3 - 63K^2 + 54K - \frac{81}{4} + \frac{1}{4} e^{-4K} (6K+9)^2 = 0$$

The solutions for these two cases are typical. The amplification factors are plotted in Figs. 3 and 4.

Figure 3

$$n = 3/2 \quad L = 1$$

Figure 4

$$n = 5/2 \quad L = 1$$

In Figure 3, for example, in the region to the left of the point where the two curves join there are two modes having $c_r = 0$. In the region to the right of this point there are two modes with $c_r \approx \pm 1$ having the same amplification factor. It can be seen that when $c_r \neq 0$ the amplification very quickly reaches the value it has for infinite k .

(d) Numerical Calculations

As can be seen in Figs. 3 and 4, the amplification reaches a maximum for values of k for which $c_r = 0$. If $c_r = 0$ ^{then} $S_+ = -S_-^*$ and the right hand side of Eq. (5.1) is the complex conjugate of the left hand side. The problem can then be formulated as the problem of finding the roots kc_i of the real equation

$$\text{arg} \frac{(iS_+) W_1'(iS_+) + (S_+ - 1) W_1(iS_+)}{(iS_+) W_2'(iS_+) + (S_+ - 1) W_2(iS_+)} = l\pi \quad (l = \text{integer})$$

This problem is quite suitable for machine calculation. The maximum amplification has been calculated on an IBM 7090 as a function of n . The result is shown in Fig. 5.

Figure 5

Recalling that $n^2 = \frac{1}{4} - \frac{J}{\cos^2 \theta}$, $J < 0$, we see that $\theta \rightarrow 90^\circ$ as $n \rightarrow \infty$. From Fig. 4 it is seen that $\alpha c_i \rightarrow \sqrt{J}$ as $n \rightarrow \infty$. This is to be expected since perturbations at right angles to the flow should not be affected by it, and the maximum amplification for the layer without a shear flow is $\alpha c_i = \sqrt{J}$ (corresponding to $k = \infty$).

Since $\alpha c_i > \sqrt{J}$ for $n < .55$ we find a critical Richardson number $(-J)_{crit} = .05$ below which the maximum instability occurs for $\cos \theta = 1$, i.e., perturbations in the windward direction, and above which the least stable mode is at right angles to the wind. Thus, the instability is of the shear type or a pure roll depending on the Richardson number. The wave number at which the maximum amplification occurs is given as a function of n in Fig. 6.

Figure 6

Wave Number of Maximum Amplification

For small n it approaches .4 which is characteristic of the velocity profile, for large n it approaches infinity which is characteristic of a convective layer.

6. THE CASE $L > 1$

If $c_r = 0$ the right hand side of Eq. (4.1) is equal to the complex conjugate of the left hand side and roots can be found without much difficulty by machine calculation as in section 5. A typical graph is shown in Fig. 7 where $\alpha c_i / \sqrt{J}$ vs k is given for $n = 1.5$ and $L = 10$.

Figure 7

$n = 1.5$ $L = 10$

The maximum amplification rates with $c_r = 0$ have been calculated for $L = 10$ and 100 and are shown in Fig. 5. The curves are qualitatively the same as for $L = 1$. The line $\alpha c_r / \sqrt{J} = 1$ is crossed at $n = .56$ for both $L = 10$ and $L = 100$ giving a critical Richardson number of $(-J) \text{ crit.} = .06$.

The wave number at which maximum amplification occurs is shown in Fig. 6 for $L = 10$. There is a discontinuity in this graph because for $n > .67$ the maximum occurs in the first loop (Fig. 7) while for $n < .67$ the maximum occurs in the second loop in a range of larger wave numbers.

7. CONCLUSIONS

The maximum instabilities have been calculated for a velocity profile in a convectively unstable layer whose width is 1 , 10 , and 100 times the width of the profile. In the latter two cases the solution is incomplete since only those modes having a wave velocity equal to the mean velocity at the center of the layer ($c_r = 0$) have been calculated. The solution for the case $L = 1$, however, indicates that the maximum instability should be among these modes. The instabilities are of the shear type or the roll type depending on a critical Richardson number which is quite insensitive to the width of the layer.

This division into shear and roll motions is somewhat unexpected, especially in view of the inequality (3.1). Instead, it might have been expected that the shear and convective instabilities would combine to give a maximum at some intermediate angle.

The use of the half-jet profile is rather unrealistic for the atmosphere where the jet type profile is characteristic⁴. It has been used because the jet profile leads to a much more difficult problem for machine computation, that of finding the complex roots of a complex equation.

Acknowledgements

I am grateful to Professors C. C. Lin and L. N. Howard for many valuable discussions throughout the course of the work.

This work was supported in part by the Office of Naval Research and in part under grant NSG 586 of the Space Nuclear Propulsion Office of the National Aeronautics and Space Administration and the Atomic Energy Commission. The numerical work was done at the computation Center at MIT, Cambridge, Massachusetts.

FOOTNOTES

1. H. L. Kuo, Phys. Fluids 6, 195 (1963).
2. A. Eliassen, E. Hoiland, and E. Riis, Institute of Weather and Climate Research, Norwegian Acad. Sci Letters, Publ. No. 1 (1953).
3. K. M. Case, Phys. Fluids 3, 366 (1960).
4. J. Kuettner, Tellus 11, 267 (1959).
5. L. N. Howard, J. Fluid Mech. 10, 509 (1961).

CAPTIONS

- Figure 1. Piecewise linear velocity profile in a layer of width $2L$.
- Figure 2. Amplification as a function of the wave number for $n = 0.9$, $L = 1$.
- Figure 3. Amplification as a function of the wave number for $n = 1.5$, $L = 1$.
- Figure 4. Amplification as a function of the wave number for $n = 2.5$, $L = 1$.
- Figure 5. Maximum amplification as a function of n for $L = 1, 10, 100$.
- Figure 6. Wave number of maximum amplification as a function of n for $L = 1, 10$.
- Figure 7. Amplification as a function of the wave number for $n = 1.5$, $L = 10$.

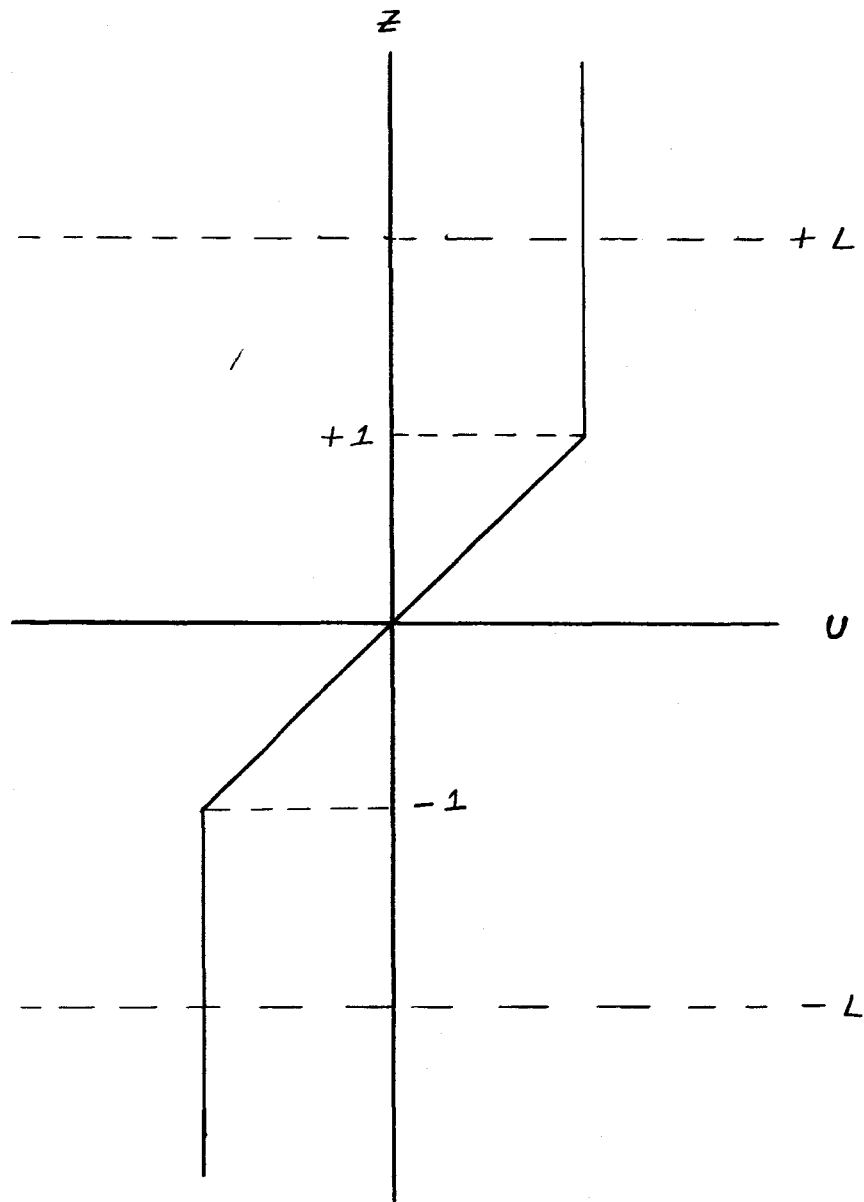


Figure 1

Piecewise linear velocity profile in a layer of width $2L$

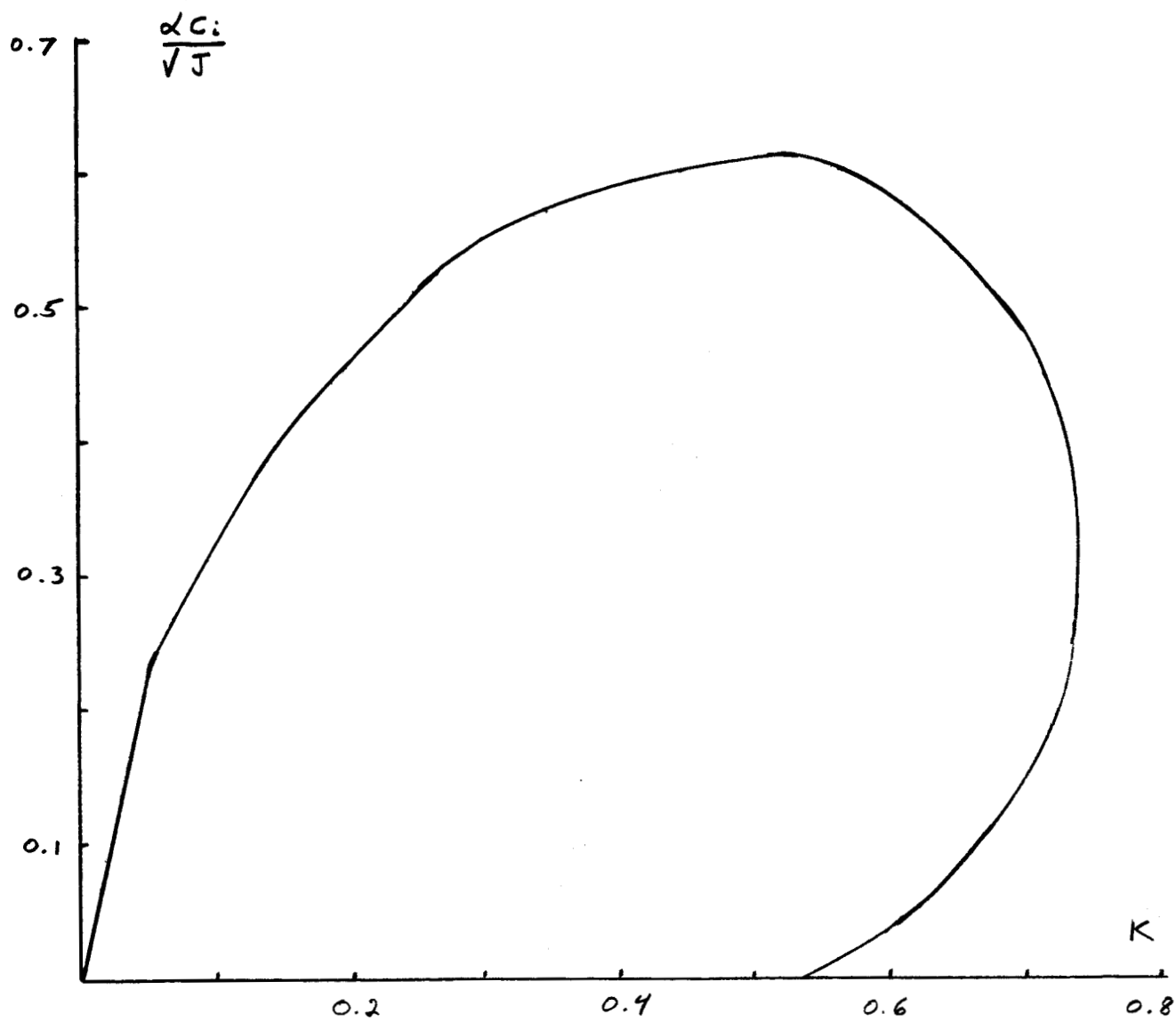


Figure 2

Amplification as a function of the wave number for $n = 0.9$, $L = 1$.

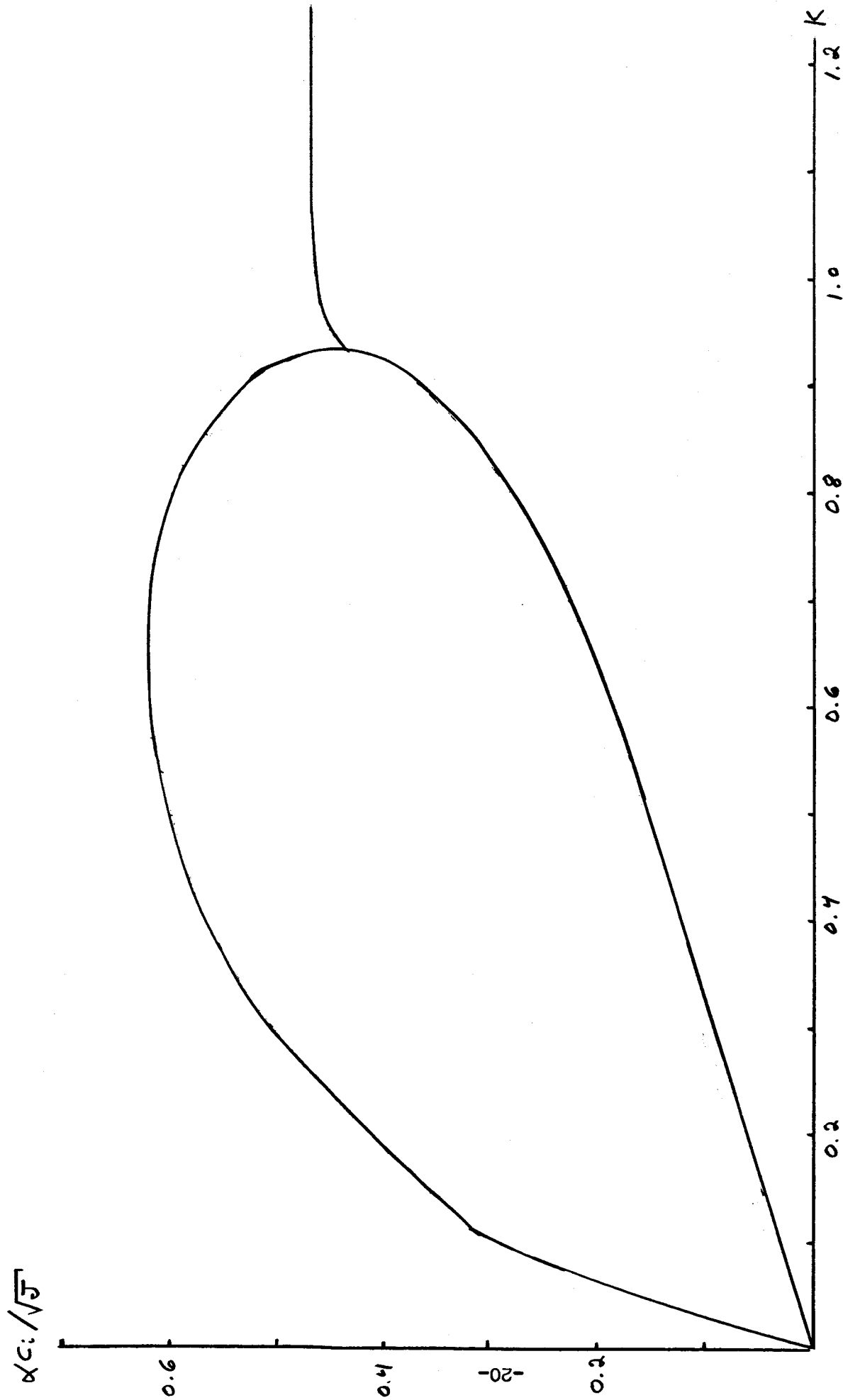


Figure 3

Amplification as a function of the wave number for $n = 1.5$, $L = 1$.

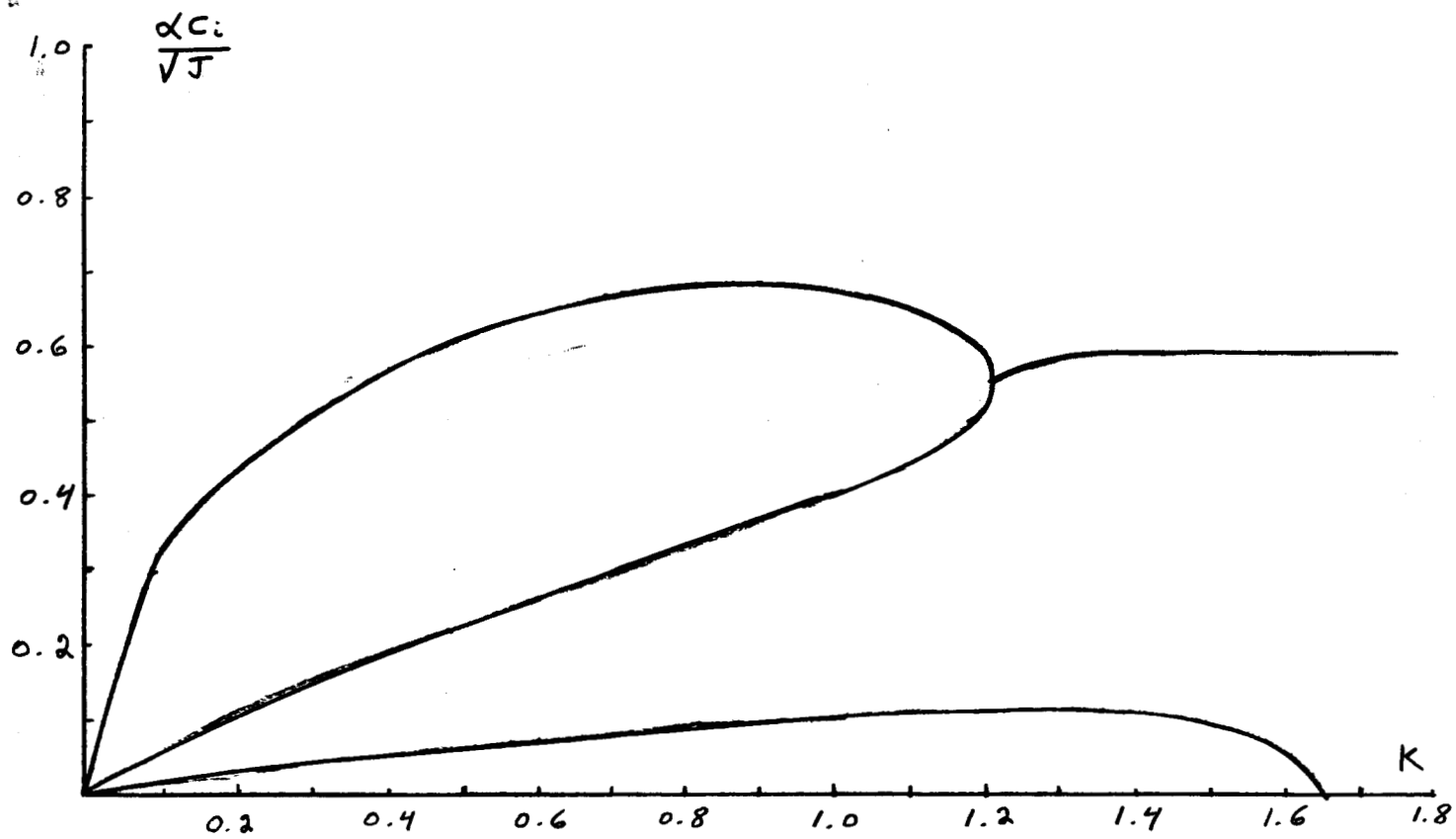


Figure 4

Amplification as a function of the wave number for $n = 2.5$, $L = 1$.

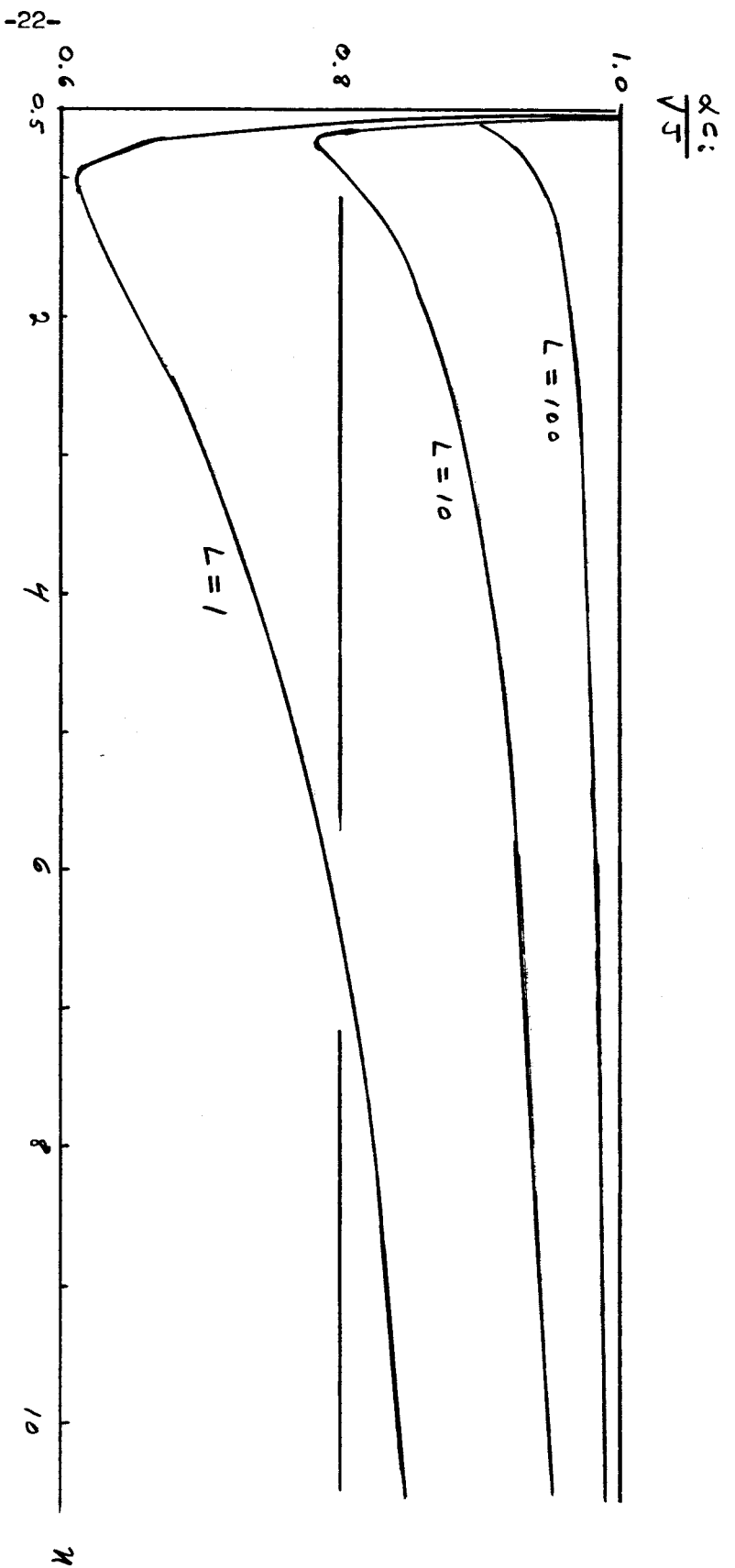


Figure 5

Maximum amplification as a function of n
for $L = 1, 10, 100$.

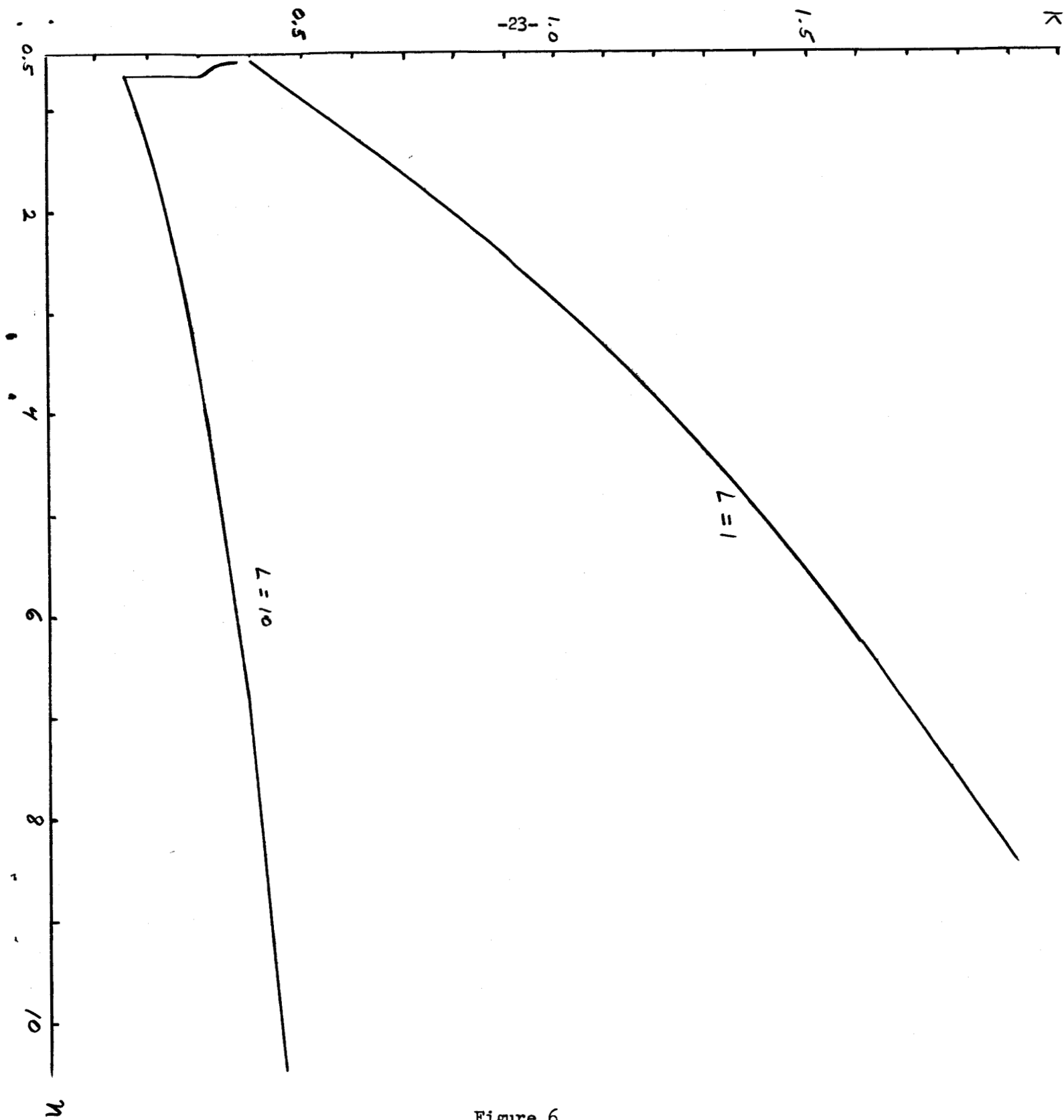


Figure 6

Wave number of maximum amplification as a function of n for $L = 1, 10$.

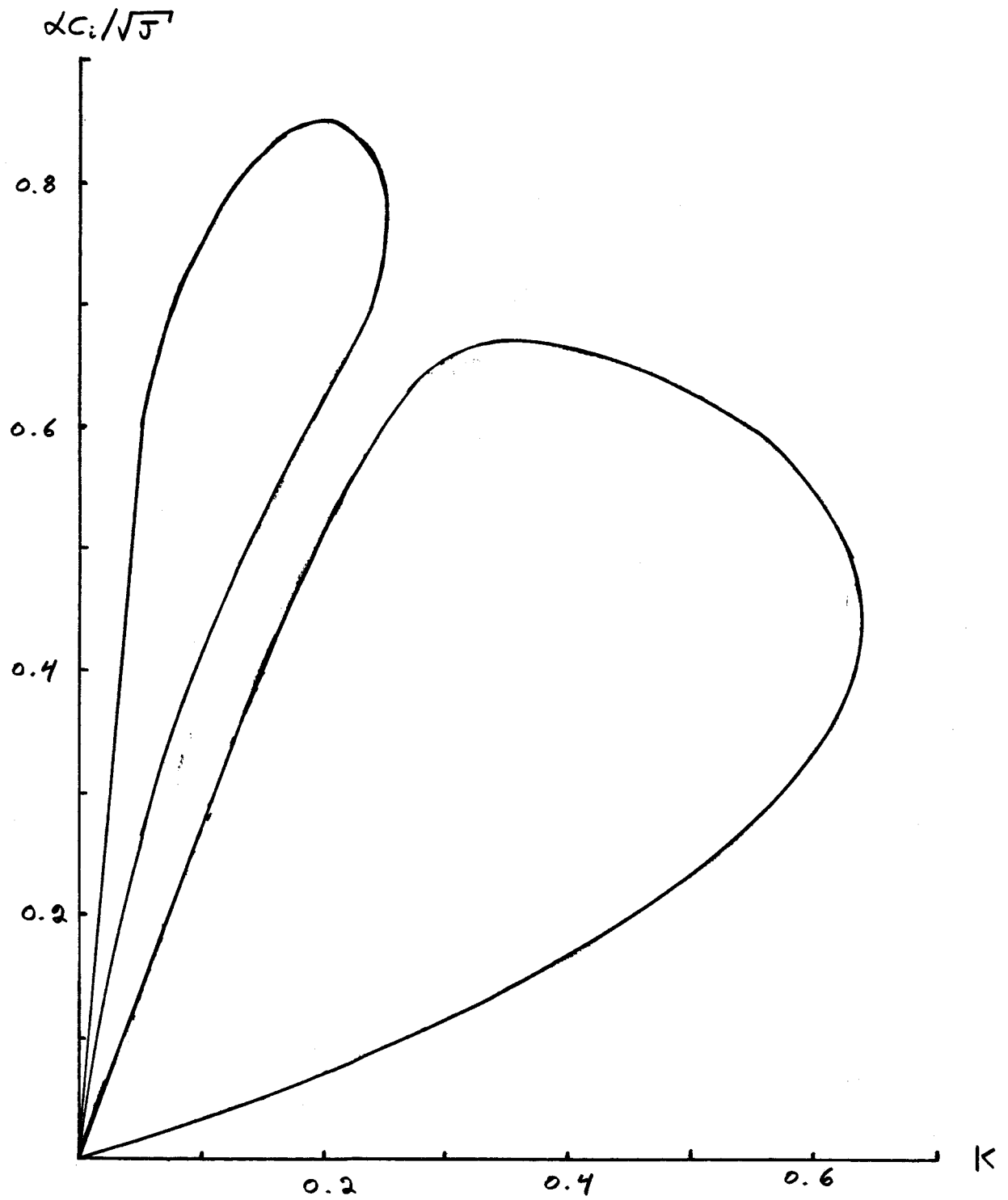


Figure 7

Amplification as a function of the wave number for $n = 1.5$, $L = 10$.